BIOCHEMISTRY
including biophysical chemistry & molecular biology

Article

pubs.acs.org/biochemistry

Cationic Copper(II) Porphyrins Intercalate into Domains of Double-Stranded RNA

Breeze N. Briggs,[†] Abby J. Gaier,[†] Phillip E. Fanwick,[†] Dilek K. Dogutan,[‡] and David R. McMillin*[,†]

[†]Purdue University, 560 Oval Drive, West Lafayette, Indiana 47907, United States

[‡]Massachusetts Institute of Technology, 77 Massachusetts Avenue, Cambridge, Massachusetts 02139, United States

Supporting Information

ABSTRACT: A cationic, copper(II)-containing ligand, derived from bulky 5,10,15,20-tetrakis(*N*-methylpyridinium-4-yl)porphyrin, Cu(T4), and two sterically friendlier forms, [*trans*-5,15-di(*N*-methylpyridinium-4-yl)-porphyrinato]copper(II), Cu(*t*D4), and [*cis*-5,10-di(*N*-methylpyridinium-4-yl)porphyrinato]copper(II), Cu(*c*D4), bind to DNA and RNA hosts. Six hairpin-forming RNA 18-mer sequences and two previously studied DNA analogues serve as convenient binding platforms of programmable base composition. A crystal structure shows that the copper center of Cu(*t*D4) is four-coordinate, establishing compatibility with intercalative binding as well as susceptibility to solvent-induced emission quenching. From the hypochromic responses and the induced emission intensities obtained with all three porphyrins, it is clear that internalization into the RNA host occurs, irrespective of the base pair composition. Further analysis reveals that the porphyrins intercalate into the double-stranded stem domains. Subtle geometric and/or electronic aspects of the binding account for the signs of induced circular dichroic signals and splitting of the Soret band of Cu(*t*D4).

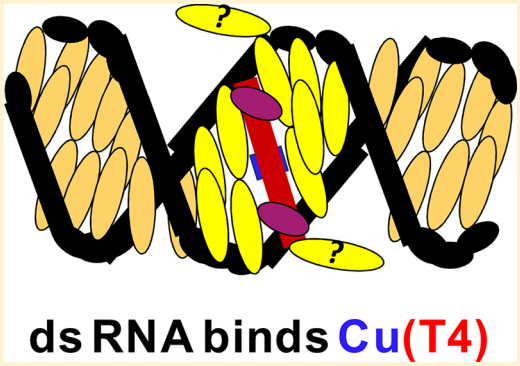

The aims of this work have been to explore binding interactions of cationic porphyrins with double-stranded (ds) RNA, as a function of the base composition of the host as well as the steric demands of the porphyrin ligand. Many previous studies have focused on binding studies with B-form DNA, especially with commercially available 5,10,15,20-tetrakis(*N*-methylpyridinium-4-yl)porphyrin (H_2T4 in Chart 1) as the ligand. The interest stems from a long list of envisioned practical applications in numerous contexts, including photodynamic therapy,[1,2] treatment of bacterial infections,[3] intracellular imaging,[4] and cancer therapy through the inhibition of telomerase.[5] The DNA binding properties of H_2T4 are also of fundamental interest because the base dependence is quite marked. Even the earliest reports revealed that H_2T4 intercalates into G≡C rich DNA sequences[6] and binds externally to A=T rich sequences.[7] In some instances, cationic porphyrins are also capable of self-stacking along the surface of the DNA host.[8] Subsequent studies have confirmed the existence of all three modes of binding.[9−12] By comparison, there is limited information available about the mode by which cationic porphyrins interact with RNA. One reason is that RNA is a complicated target that adopts a globular structure complete with a secondary structure that includes, for example, helical segments stabilized by base stacking interactions. The chain can also fold back on itself and gives rise to base pairing interactions, the formation of double strands, and the appearance of stem−loop, or hairpin, structures.[13] Double-stranded RNA structures have many uses as recognition elements,[14,15] in the realm of RNAi and natural antiviral response mechanisms,[16,17] and in the design of new therapies for targeting RNA viruses like HIV.[18,19] A possible limitation is that the literature suggests that intercalators bind less strongly to double-stranded RNA by comparison with its DNA cousin.[20] However, data are sparse because only a few strictly double-stranded sequences of RNA are routinely available, including the often used poly(rA)·poly(rU) and poly(rG)·poly(rC) systems.[21−24]

Chart 1

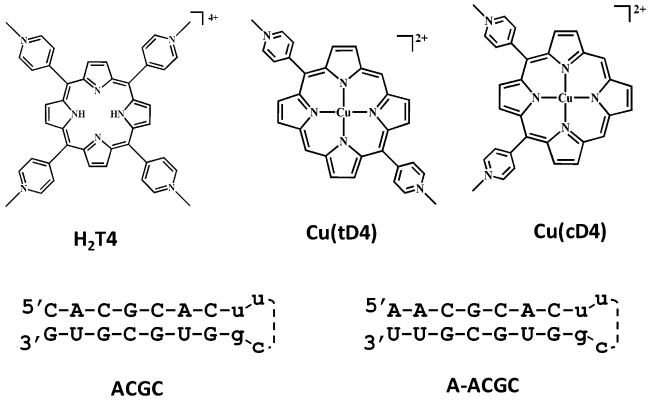

Received: June 20, 2012
Revised: August 31, 2012
Published: September 4, 2012

Hairpin structures serve as an alternative source of double-stranded RNA hosts. The long-recognized stability of the hairpin platform has led to its use in many DNA-based studies, including investigations of long-range electron-transfer processes,[25] sensing applications involving molecular beacons,[26] and DNA binding studies.[27−31] Of course, RNA hairpins have also been useful in binding studies.[32,33] Hairpin structures are convenient because they form readily and are thermally stable because of the intramolecular character of base pairing. Closing C≡G base pairs at the stem ends further bolster stability. When the loop end is relatively large and involves many bases, it can also act as a binding domain.[15,34] However, naturally occurring RNA hairpins often feature a tight CuucgG loop turn, where lowercase letters denote non-Watson−Crick hydrogen-bonded residues.[14,35] At the same time, the comparatively extended stem domain, which defines a classical A-form double helix, complete with identifiable broad minor and comparatively deep major grooves,[36] is an ideal compartment for ligand binding. Key to the utility of the design, the residues within the stem are easy to vary, determine the rigidity of the framework, and largely define the electrical field that emanates from the host.

Variations in the ligand or the host are important because they affect steric considerations and the charge distribution. Compared with a B-form double helix, the major groove of an A-form duplex is comparatively narrow, deep, and suffused with phosphate groups, while the minor groove is broad, shallow, and sprinkled with hydroxyl groups.[37,38] When the porphyrin binds to B-form DNA, its steric demands can come into play because intercalation of H_2T4 entails inserting two bulky substituent groups into the minor groove, where clashes with the sugar phosphate backbone occur.[39] Intercalation is less problematic with sterically friendly analogues of H_2T4, especially 5,15-di(*N*-methylpyridinium-3-yl)porphyrin,[40,41] 5,15-di(*N*-methylpyridinium-4-yl)porphyrin (H_2*t*D4),[41] and 5,15-dimethyl-10,20-di(*N*-methylpyridinium-4-yl)porphyrin (H_2*t*Me$_2$D4).[42] See Chart 1 for a view of the copper(II) forms and abbreviations. Intercalation of H_2*t*D4 or H_2*t*Me$_2$D4 is comparatively easy as it involves inserting only one bulky substituent into the minor groove; hence, the latter porphyrins intercalate into DNA regardless of what base pairs are present.[41,42] Other workers have also explored similar systems.[34,43,44] The new derivative 5,10-di(*N*-methylpyridinium-4-yl)porphyrin (H_2*c*D4) studied here is no less intriguing because intercalation can occur with the two substituents in the same or opposite grooves, whichever option is more favorable. Employing the copper(II) forms Cu(*t*D4) and Cu(*c*D4) (Chart 1) is advantageous because the emission signal is diagnostic of the binding motif.[12,42,45] On the other hand, interpreting the induced circular dichroism (CD) spectrum, which is traditionally quite useful for DNA binding studies,[10,11] proves to be less straightforward.

EXPERIMENTAL PROCEDURES

Materials. Used as received chemicals typically were products of one of two suppliers. In particular, the supplier of dichlorodimethylsilane, acetonitrile (MeCN), iodomethane, tetrabutylammonium nitrate, methanol, copper acetate [Cu(OAc)$_2$], KPF$_6$, 2,3-dichloro-5,6-dicyano-1,4-benzoquinone (DDQ), acridine orange, Trizma HCl, Trizma base, silica and alumina TLC plates, and H_2T4(PTS)$_4$, where PTS denotes *p*-tolylsulfonate, was Sigma Aldrich. The supplier of the solvents dimethylformamide (DMF), acetone, dichloromethane (DCM), and hexane, as well as HCl(aq), diisopropylamine, KNO_3, and nitric acid (HNO_3), was Mallinckrodt. The RNA hairpins and TEMED-acetate buffer were from Dharmacon Inc. TEMED is *N*,*N*,*N*′,*N*′-tetramethylethylene diamine.

Methods. Silanization of the cuvettes and selected other glassware was necessary to minimize absorption of the cationic porphyrins.[46] Preparation of the 0.05 M Tris buffer (pH 7.5) entailed adding enough Trizma HCl to deionized water so that the final concentration was 0.05 M after the pH had been adjusted with a concentrated solution of Trizma base in deionized water and dilution to the final volume with water. Another step for buffers prior to their use in solutions containing RNA involved autoclaving for 2 h.

Dicationic Porphyrins. The preparations of 5,10-*cis*-di(pyrid-4-yl)porphyrin and 5,15-*trans*-di(pyrid-4-yl)porphyrin followed literature procedures.[41,47] Preparations of 5,10-*cis*-di(pyrid-4-yl)porphyrin frequently exhibited an anomaly in the excitation of the porphyrin at 645 nm where the chlorin derivative absorbs. Serial additions of small aliquots of a solution containing DDQ help avoid overoxidation and serve to reduce the absorption intensity 645 nm in favor of the desired band at 635. Treatment of 100 mg (0.22 mmol) of the *cis* porphyrin with DDQ (0.05 g, 0.22 mmol) gave the final product after batch elution from florisil with 1% MeOH in DCM. The total recovery was only 25 mg of clean material, however. DDQ and byproducts stayed with the resin.

Methylation of Porphyrin and Copper Insertion. The procedure used for methylation of 5,10-*cis*-di(pyrid-4-yl)-porphyrin is representative of those used for the *trans* analogue, as well as commercially obtained H_2T4[PTS]$_4$, and is similar to one reported previously.[42] See the Supporting Information. Methylation of the commercial material was necessary because thin layer chromatography (TLC) revealed the presence of multiple charge states.[48] The procedure used for inserting copper(II) into H_2*c*D4 was similar to those used for the preparations of Cu(T4) and Cu(*t*D4). See the Supporting Information for details. For all copper porphyrins used in this study, the most difficult-to-remove impurity is a trace of the zinc(II) analogue that forms as a result of adventitious zinc salts that can come from more than one source. Pure preparations of copper-containing porphyrins always elute as one band on TLC plates and exhibit negligible emission in aqueous solution.

X-ray Structure. A fiber served to mount a red needle of $C_{32}H_{24}CuN_6{\cdot}2(C_7H_7O_3S){\cdot}CH_3OH$ having approximate dimensions of 0.20 mm × 0.10 mm × 0.02 mm in a random orientation. Least-squares refinement, using the setting angles of 50251 reflections in the 3° < q < 66° range, yielded cell constants for data collection. The Patterson heavy-atom method allowed determination of the structure and initially revealed the position of the Cu atom. Succeeding difference Fourier syntheses located the positions of the remaining atoms. The refinement included hydrogen atoms constrained to ride on preselected atoms. For full-matrix least-squares refinement, the function minimized was $\sum w(|F_o|^2 - |F_c|^2)^2$, with the weight w defined as $1/[\sigma^2(F_o^2) + (0.0753P)^2 + 0.0000P]$, where $P = (F_o^2 + 2F_c^2)/3$. The refinement utilized 6533 reflections; however, the calculation of R1 involved only the 4328 reflections for which $F_o^2 > 2\sigma(F_o^2)$. The final cycle of refinement included 575 variable parameters. The goodness of fit was 1.18. The highest peak in the final difference Fourier had a height of 0.74 e/Å^3. The minimal negative peak had a height of −0.88 e/Å^3.

dx.doi.org/10.1021/bi300828z | *Biochemistry* 2012, 51, 7496−7505

The copper compound is isostructural with the metal-free $[H_2D4](PTS)_2{\cdot}CH_3OH$ analogue reported previously.[45] Unit cell parameters for the copper structure are listed in Table 1.

Table 1. Crystallographic Data for $C_{32}H_{24}CuN_6{\cdot}2(C_7H_7O_3S){\cdot}CH_3OH$

$C_{47}H_{42}CuN_6O_7S_2$	930.56
a = 27.7209(19) Å	space group $P2_{1/c}$
b = 8.8460(2) Å	T = 150(1)
c = 17.4420(3) Å	$\lambda_{CuK\alpha}$ = 1.54184
β = 105.179(7)°	ρ_{calcd} = 1.497 g cm^{-3}
V = 4127.9(3) Å^3	μ_{ave} = 2.212 mm^{-1}
R1 = 0.060 $[I > 2\sigma(I)]^a$	wR2 = 0.135 $[I > 2\sigma(I)]^b$
transmission coefficient = 0.609−0.957	

^{a}R1 = $\sum||F_o| - |F_c||/\sum|F_o|$ for $F_o^2 > 2\sigma(F_o^2)$. ^{b}wR2 = $[\sum w(|F_o^2| - |F_c^2|)^2/\sum w|F_o^2|^2]^{1/2}$.

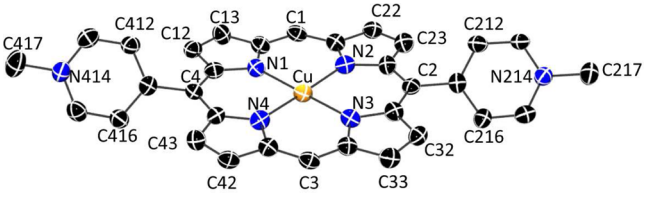

Figure 1. Representation of the cation in $[Cu(tD4)](TPS)_2{\cdot}CH_3OH$ with thermal ellipsoids set at 50% probability. Hydrogen atoms have been omitted for the sake of clarity.

Figure 1 shows a representation of the Cu(tD4) cation found in the asymmetric unit. The porphyrin core is approximately planar but exhibits a hint of a ruffling distortion. Thus, alternating pyrrole rings tend to cant in opposite directions relative to the mean plane of the porphyrin. Also, the *meso* carbons deviate from the mean plane farther than the β carbons of the pyrrole groups on average. The N214 and N414 pyridine rings twist out of the plane, forming dihedral angles of 57.0° and 53.0°, respectively.

RNA and DNA Hosts. Synthetic RNA from Dharmacon comes with protecting groups on to prevent degradation of the material. The method for deprotection requires treating the RNA pellet with 400 μL of a 100 mM TEMED-acetate buffer (pH 3.8) for 30 min at 60 °C. Subsequent steps involved evaporation of the buffer, ethylene glycol, and formic acid with a SpeedVac and then storage of the resulting RNA pellet in a freezer at −10 °C. Introduction into autoclaved μ = 0.05 M Tris buffer (pH 7.5) produced the RNA stock solution used in spectral titrations. By invoking the nearest-neighbor approximation,[49] Dharmacon supplied calculated molar absorptivities that were useful for quantifying RNA concentrations in units of base pairs. See Table 2 for the hairpin sequences employed, abbreviations used, and physical data. The DNA hairpins CG[t_4] and TT[t_4] were available from previous studies.

Chart 1 also presents a schematic view of representative RNA hosts. Every host has a 5′-uucg-3′ loop preceded by a closing C≡G base pair preceded in turn by an A═U base pair. The closing base pair at the opposite end of the stem is usually a C≡G base pair. The variable sequence between the ends suggests the abbreviated name. For example, ACGC in the chart has that run of bases between C_1 and A_6 in the hairpin sequence. Two of the hairpins have a closing A═U base pair with A at the 5′ end and U at the 3′ end of the sequence. The abbreviated name is then A-ACGC (see Chart 1).

Table 2. RNA Hosts

abbreviation	stem	loop	ε (mM^{-1} cm^{-1})
ACGC	5′-CACGCAC	5′-uu	18.4
	3′-GUGCGUG	3′-cg	
GACG	5′-CGACGAC	5′-uu	18.8
	3′-GCUGCUG	3′-cg	
AUGU	5′-CAUGUAC	5′-uu	19.9
	3′-GUACAUG	3′-cg	
AUAU	5′-CAUAUAC	5′-uu	20.7
	3′-GUAUAUG	3′-cg	
A-ACGC	5′-AACGCAC	5′-uu	19.0
	3′-UUGCGUG	3′-cg	
A-GUAU	5′-AGUAUAC	5′-uu	20.8
	3′-UCAUAUG	3′-cg	
CG[t_4] (DNA)	5′-d(GACGAC)	5′-d(tt)	13.6
	3′-d(CTGCTG)	3′-d(tt)	
TT[t_4] (DNA)	5′-d(GATTAC)	5′-d(tt)	17.8
	5′-d(CTAATG)	3′-d(tt)	

Titrations. To ensure disaggregation of the porphyrin, the medium used for measuring spectra of Cu(cD4) or Cu(tD4) in the absence of RNA contained 50% Tris buffer and 50% MeOH (see the Supporting Information for studies of the influence of MeOH). However, when RNA was present in the sample, the only source of MeOH was a negligible amount introduced with the porphyrin stock solution that was 50% by volume MeOH. Via introduction of more porphyrin along with each aliquot of RNA stock solution, it was possible to maintain the porphyrin concentration constant as q, the RNA base pair:porphyrin concentration ratio, increased.

The molar absorptivity of acridine orange (51000 M^{-1} cm^{-1}) is relatively low.[50] Therefore, to conserve RNA in titration experiments, the small-volume cuvette used for absorbance and CD studies of the dye had a path length of 5.0 cm. Cuvettes used for emission measurements always had a path length of 1.0 cm; however, the absorbance at the excitation wavelength often changed during titrations. Dividing the emission intensity at each wavelength λ by the fraction of light absorbed ($1 - 10^{-A'}$), where A' denotes the absorbance at the excitation wavelength, effectively compensates for absorbance differences and facilitates comparisons between runs.[51] In the case of circular dichroism (CD) measurements, multiplying the as-recorded signal in millidegrees by $(Qcl)^{-1}$, where Q equals 32980, c is the molar concentration of the chromophore, and l is the path length in centimeters, converted the scale to $\Delta\varepsilon$ units. A Beer's law plot obtained from predetermined masses of crystalline $[Cu(tD4)](TPS)_2{\cdot}CH_3OH$ in conjunction with standard volumetric methods yielded a molar absorbance value of 137000 M^{-1} cm^{-1} for Cu(tD4) in a 50:50 (v/v) MeOH mixture at 410 nm, and the same value has been used for calculating stock concentrations of Cu(cD4) that has an absorption maximum at 407 nm. The corresponding value for Cu(T4) in buffer at 424 nm is 231000 M^{-1} cm^{-1}.[52]

Instrumentation. The absorbance spectrophotometer was a Varian Cary 300 Bio instrument, while the fluorimeter used to monitor emission and excitation spectra was a Varian Cary Eclipse instrument with an R3896 phototube detector. A JASCO-J810 spectropolarimeter provided CD data. The pH meter was a Corning model 430 instrument, and the autoclave was an AMSCO 2321 Gravity Eagle Series instrument. The

diffractometer was a Rigaku Rapid II instrument equipped with confocal optics. The machine used for determining the crystal structure was a LINUX personal computer using SHELX-97.[53]

RESULTS

Cu(*t*D4) and Cu(*c*D4). The two dipyridiniumyl porphyrins behave similarly, and neither exhibits a measurable emission signal in the absence of a host. Investigations involving B-form DNA hosts provide a useful context for understanding binding-induced spectral changes. The first results involve the CG[t_4] host that is rich in cytosine-guanine base pairs and supports the intercalation of even bulky porphyrins like H_2T4 and Cu(T4).[10,12,45] Consistent with that same mode of binding, uptake of Cu(*t*D4) induces a hypochromic response ($H > 0$) along with a negative CD signal in the Soret region. Importantly, a photoluminescence signal also appears at longer wavelengths (Figure 2). Table 3 reveals that Cu(*c*D4) gives

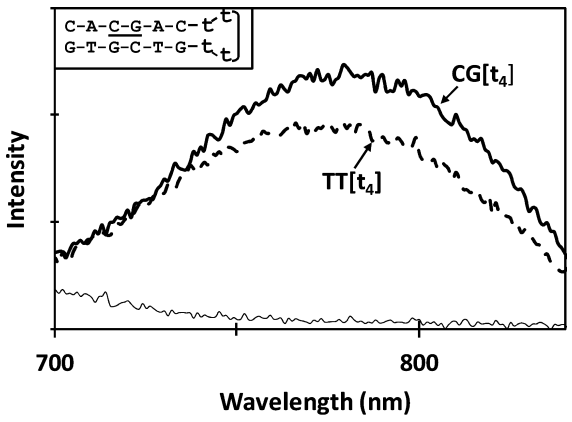

Figure 2. Emission spectra of 2.3 μM Cu(*t*D4) in a 50% (v/v) methanol buffer solution (thin solid line) as well as in a buffer solution in the presence of the DNA hairpins CG[t_4] (thick solid line) and TT[t_4] (dashed line), at $q = 27$ in each case. The inset shows the CG[t_4] DNA hairpin with naming residues underlined.

similar results. The A═T rich TT[t_4] host represents another key comparison because the duplex structure is much less rigid, and bulky ligands like Cu(T4) preferentially bind to it externally.[27,28] Here again, however, data presented in Figure 2 and Table 3 clearly show that sterically friendly Cu(*t*D4) and Cu(*c*D4) strictly intercalate into TT[t_4]. The Cu(*t*D4) system is unusual in that the Soret band becomes broader and nearly splits into two transitions upon binding. Figure 3 shows absorption spectra obtained in the presence and absence of an excess of the TT[t_4] host. When the porphyrin binds to TT[t_4], the lower-energy component absorbs more strongly, and the same effect occurs with binding to CG[t_4]. On the other hand, the higher-energy component is dominant in the induced CD spectrum, which Figure 3 also illustrates.

Except for the sign of the induced CD signal, vide infra, exposing the dipyridiniumyl porphyrins to RNA hairpins induces very similar responses, including the splitting of the Soret absorption of Cu(*t*D4). Here the band shape varies to some extent, depending on the base composition. For example, when the host is ACGC, the Soret absorption skews slightly toward shorter wavelengths, but Figure 4 reveals greater intensity on the longer wavelength side when the host is AUAU. The band shape actually changes during a titration with AUAU in that the absorbance is more intense on the short-

Table 3. Physical Data

					CD	
RNA/DNA	% GC	$\Delta\lambda$ (nm)	% H	I'	λ (nm)	$\Delta\varepsilon$ (M^{-1} cm^{-1})
Cu(*c*D4)						
ACGC	72	13	46	5.0	421	+12
A-ACGC	57	13	44	6.0	420	+14
AUGU	42	16	30	2.5	415	+6
AUAU	28	15	32	2.5	416	+8
A-GUAU	28	16	35	2.5	416	+7
CG[t_4][a]	50	15	33	2.0	428	−11
TT[t_4][a]	25	16	36	4.0	426	−15
Cu(*t*D4)						
ACGC	72	15	48	5.0	420	+17
AUGU	42	14	42	3.3	420	+16
AUAU	28	16	20	2.3	420	+9
CG[t_4][a]	50	16	28	4.8	414	−10
TT[t_4][a]	25	16	24	3.7	415	−20
Cu(T4)						
ACGC	72	9	32	3.8	424	+6
					445	−10
GACG	72	10	30	3.5	424	+7
					445	−8
AUGU	42	9	24	2.8	438	−6
AUAU	28	10	23	1.6	436	−9
A-GUAU	28	10	16	2.8	438	−9
CG[t_4][a]	50	10	34	2.3	436	−29
TT[t_4][a]	25	5	2	<0.5	420	+15

[a]DNA host.

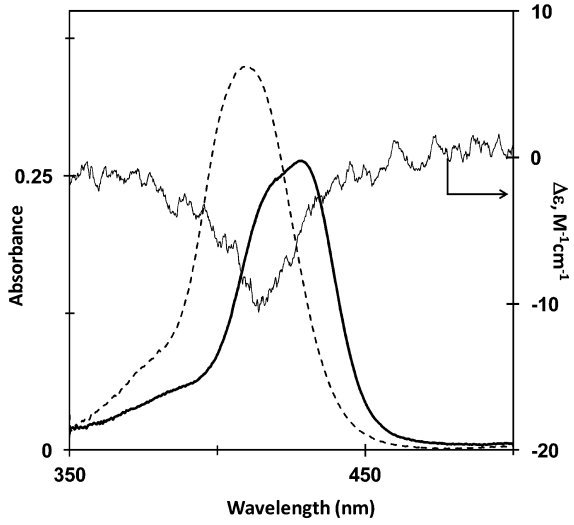

Figure 3. Absorption spectra of 2.3 μM Cu(*t*D4) at $q = 0$ (dashed line) and in the presence of the DNA hairpin TT[t_4] at $q = 27$ (thick solid line). The thin solid line is the corresponding induced CD spectrum. Both signals represent limiting spectra.

wavelength side of the band at low q values. On the other hand, in the presence of an excess of the AUAU host, the CD spectrum is broad and shows no detectable asymmetry, within the limit imposed by the signal-to-noise ratio (see Figure 4).

As a whole, the results for dipyridiniumyl porphyrins do not vary greatly with the base content of the RNA host, though they cluster into two sets. In particular, the G≡C rich hosts ACGC and A-ACGC induce slightly weaker bathochromic responses ($\Delta\lambda$), but more hypochromism and stronger emission signals (I'). Figure S2 of the Supporting Information

dx.doi.org/10.1021/bi300828z | *Biochemistry* 2012, 51, 7496−7505

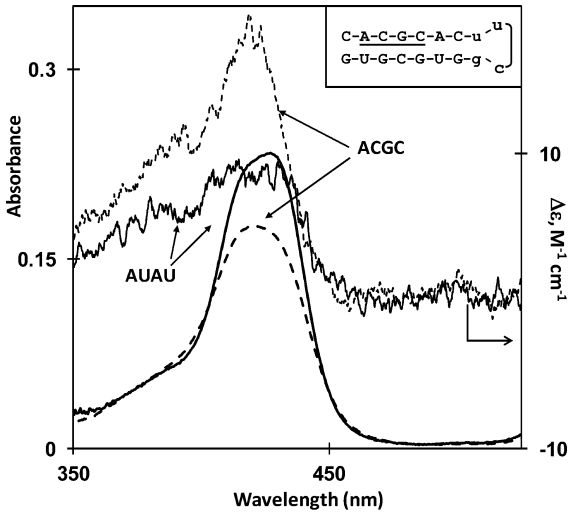

Figure 4. Limiting absorption spectra obtained in buffer at q = 46 during titrations of 2.3 μM Cu(*t*D4) with the RNA hosts AUAU (thick solid line) and ACGC (dashed line). Corresponding CD spectra appear as the top traces. The inset shows the ACGC RNA hairpin with naming residues underlined.

presents a comparison of two emission signals from bound forms of Cu(*c*D4). See Figure 5 for a comparison of CD spectra

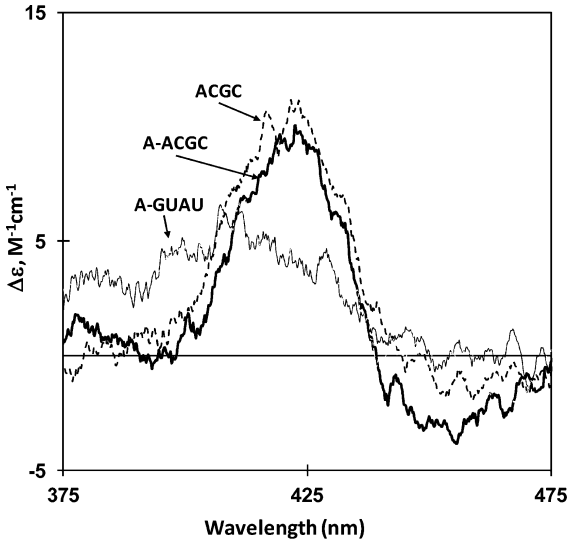

Figure 5. Induced CD spectrum of Cu(*c*D4) bound to the RNA hairpin: ACGC (dashed line), A-ACGC (thick solid line), and A-GUAU (thin solid line), all limiting spectra obtained at q = 39. The spectrum obtained with AUAU virtually overlays that of A-GUAU.

of Cu(*c*D4) bound to different RNA hosts. It is clear that G≡C rich sequences induce a stronger response in the Soret region. On the other hand, interaction with A═U rich hosts induces more CD intensity in the vicinity of 380 nm, which may relate to a shoulder found in the absorption spectrum. The one striking difference vis-à-vis DNA binding is that RNA hosts induce a positive CD signal in the Soret region.

It is important to note that the results in Table 3 describe limiting spectra obtained at high base pair:ligand ratios. At earlier stages in a titration, significantly different spectral perturbations are sometimes evident. For example, Figures 6 and 7 illustrate results obtained in the course of adding A-

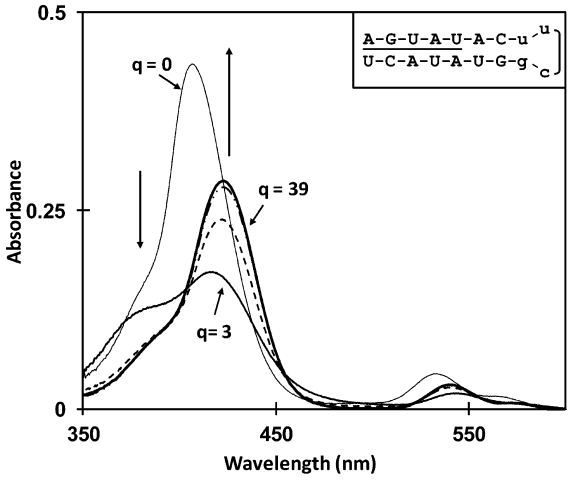

Figure 6. Absorbance-monitored titration of the RNA host A-GUAU into a buffer solution containing 2.3 μM Cu(*c*D4). The spectra relate to solutions containing RNA at q = 0 (thin solid line, in 50% methanol), q = 3 (medium solid line), q = 15 (dashed line), q = 31 (dashed−dotted line), and q = 39 (thick solid line). The inset is a representation of the A-GUAU RNA hairpin with naming residues underlined.

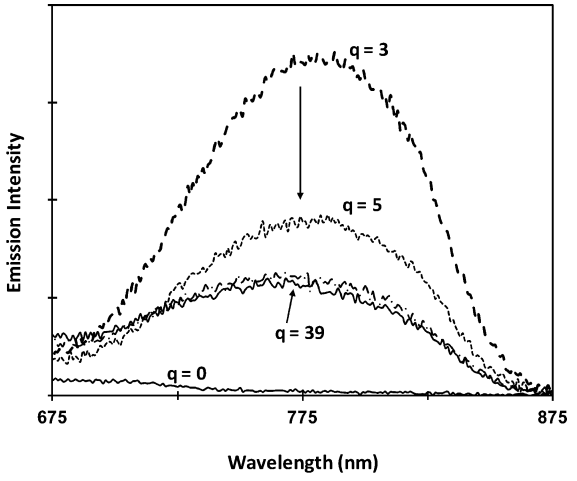

Figure 7. Emission monitored in a titration of the RNA host A-GUAU into a buffer solution containing 2.3 μM Cu(*c*D4). The spectra are for solutions containing RNA at q = 0 (thin solid line, in 50% methanol), q = 3 (dashed line), q = 5 (dotted line), q = 31 (dashed−dotted line), and q = 39 (thick solid line). The latter represents the limiting spectrum.

GUAU at a constant concentration of Cu(*c*D4). Note that the hypochromic response is comparatively large at higher loading (q = 3 bp/ligand), when a shoulder at ∼360 nm is also quite prominent. The same conditions also yield a stronger emission signal (Figure 7). The spectral changes then become more moderate upon addition of more RNA to the solution and achieve the tabulated, limiting values by a ratio of $q \approx 31$. Similar effects occur in DNA titrations as well. See, for example, the CD results in Figure S3 of the Supporting Information relating to the interaction of Cu(*t*D4) with TT[t_4]. The spectral changes become nonmonotonic whenever important interactions between ligands occur at high loading (vide infra). At very high loadings, external aggregation is also possible. Such complications commonly occur with dicationic porphyrins and preclude the application of simple equilibrium models.[45]

dx.doi.org/10.1021/bi300828z | *Biochemistry* 2012, 51, 7496−7505

It is nevertheless clear that arriving at the limiting spectrum requires about the same q value for a dipyridiniumyl porphyrin or Cu(T4), whether the host is RNA or DNA. Thus, the equilibrium constant for dissociation of the porphyrin is on the order of 10^{-6} to 10^{-7} M, gauged in terms of the concentration of base pairs of the host.[54,55]

Cu(T4). In comparison to those of dipyridiniumyl porphyrins, the spectra of Cu(T4) show many parallels, but more variation from one host to the next. One parallel is that the interaction of Cu(T4) with an RNA host always produces a hypochromic response and bathochromism in the Soret region. The bound porphyrin also invariably exhibits photoluminescence, and the emission intensity increases with the percentage of G≡C base pairs present in the host. Indeed, interaction with a G≡C rich RNA hairpin induces a stronger emission signal than interaction with the DNA hairpin CG[t_4]. On the other hand, a survey of Table 3 reveals that the spectral changes induced when Cu(T4) binds to an RNA host are generally less pronounced than those observed with Cu(*t*D4) or Cu(*c*D4). Another difference is that, in contrast to the behavior observed in Figure 7, the emission intensity from Cu(T4) strictly increases with the concentration of RNA host added, until the approach to the limiting spectrum. Curiously, in at least one case, the amount of RNA necessary for attaining the limiting emission signal of Cu(T4) exceeds that required for achieving the limiting absorption spectrum; see results with AUGU in Figure S4 of the Supporting Information. The most dramatic variations with base composition probably occur in the induced CD spectra. A C≡G rich host like ACGC, for example, induces a bisignate response that crosses the baseline at the wavelength where the Soret absorption maximum of Cu(T4) occurs (Figure 8). In contrast, an A═U rich hairpin like AUGU induces a strictly negative CD signal. For the most part, there is little induced CD intensity in the vicinity of 375 nm; however, a few RNA hosts, including GACG, induce a weak positive signal (Figure 8).

Acridine Orange. Studies with acridine orange interacting with DNA and RNA hairpins serve as controls and comport with literature studies involving conventional double-stranded hosts. In particular, uptake by the DNA hairpin CG[t_4] induces a hypochromic response and a limiting bathochromic shift from 494 to 502 nm in the visible absorption spectrum.

The induced CD signal is also negative (Figure 9), all results being in accordance with those of Iwamura and co-workers who studied intercalation into calf thymus DNA.[56] On the other hand, the Iwamura group also established that intercalation into double-stranded RNA induces the opposite response, i.e., a positive CD signal from the bound form of acridine orange.[50] Figure 9 shows that interaction with the RNA hairpin GACG yields a similar result.

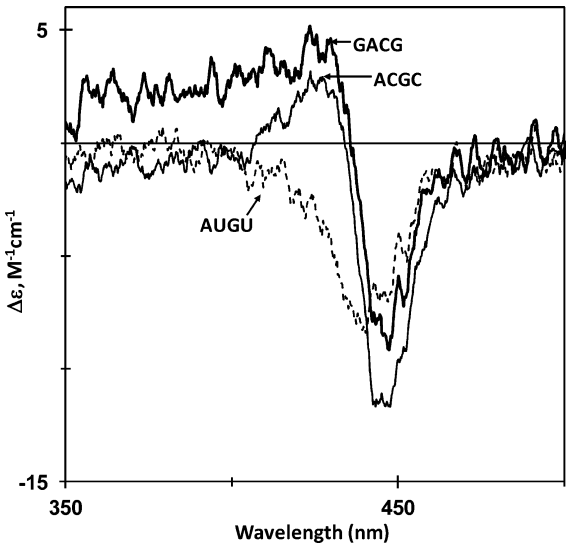

Figure 8. Induced CD spectra measured in the Soret region of Cu(T4) in the presence of G≡C rich RNA hosts GACG (thick solid line) and ACGC (thin solid line), both at q = 23, as well as A═U rich host AUGU (dashed line), at q = 31. Each is a limiting spectrum.

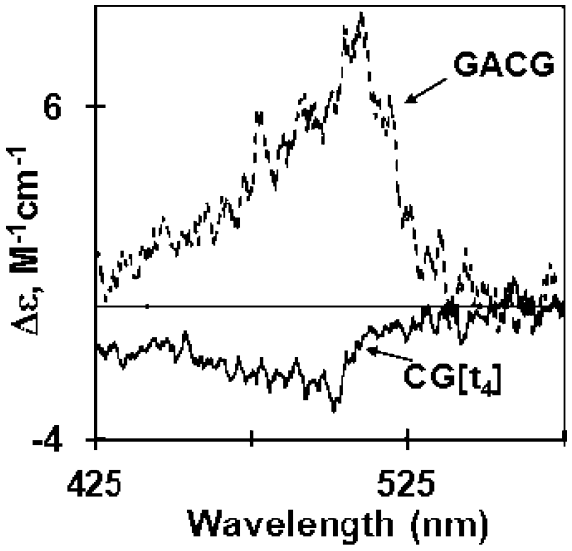

Figure 9. Induced CD spectra of acridine orange exposed to excess RNA host GACG (dashed line, at q = 46) vs DNA host CG[t_4] (solid line, at q = 39).

DISCUSSION

Previous Work, Methodology, and Choice of Ligands. Few reports of RNA binding studies with cationic porphyrins are available, and all focus on tetra-substituted systems like H_2T4. As usual, physical methods provide insight into binding interactions; however, the rules for interpreting spectral changes need not be exactly the same for DNA and RNA structures. That said, one of the more transparent methods is electronic absorbance. Internalization of the porphyrin generally entails stacking among aromatic bases, which results in a significant bathochromic shift of the Soret band as well as a strong hypochromic response.[10,12] With external binding, the bases are farther removed, bathochromic shifts are small, and there is little or no hypochromism.[10,27,57] By comparison with absorption, changes in the fluorescence of H_2T4 are minimal whether the porphyrin binds externally or by intercalation.[29,58,59] The likely reason is that the emission originates from a low-energy excited state far removed from the electronic transitions of the base residues. The interpretation of induced CD signals is more problematic because double-stranded (ds) RNA forms an A-form double helix, as opposed to the B-form structure adopted by DNA. Indeed, as emphasized earlier, intercalation of acridine orange into ds RNA induces a positive CD signal, whereas the same mode of binding to DNA induces a negative signal.[50] Fortunately, emission studies of copper(II) porphyrins are capable of providing unique information about

dx.doi.org/10.1021/bi300828z | *Biochemistry* 2012, 51, 7496−7505

the binding motif. While the $\pi-\pi^*$ photoluminescence signal obtained is orders of magnitude weaker than the fluorescence of the native porphyrin, the emission from the copper(II) form is extremely sensitive to the local environment.[12,45,57] Observation of an emission signal is good evidence of intercalation into a double-stranded host, while fully quenched emission signals external binding. The basis of the effect is that contact between the copper(II) center and a coordinating agent, such as the solvent, during the lifetime of the excited state results in emission quenching.[57]

A brief literature survey illustrates the difficulty in ascertaining binding motifs with RNA hosts. Uno et al. investigated the binding of Cu(T4) and H_2T4 to the double-stranded RNA hosts poly(rA)·poly(rU) and poly(rI)·poly(rC).[21] They observed hypochromic responses of 40% H and bathochromic $\Delta\lambda$ shifts of ~10 nm. Largely because they obtained conservative induced CD signals, they concluded that the porphyrins bind externally by self-stacking along the RNA. More recently, Ghazaryan et al. conducted additional binding studies with the same hosts.[24] Their studies included a modified form of H_2T4, termed H_2TE4 here, which differs from H_2T4 in that the R group employed in quaternizing the pyridine nitrogens is -CH_2CH_2OH rather than -CH_3. On the basis of the observed hypochromic responses (40−50%), $\Delta\lambda$ shifts, and negative induced CD signals, they concluded that H_2TE4 intercalates into both RNA hosts. However, they also determined that a bulkier porphyrin bearing isopropyl R groups adopts an external binding motif.[24] The goals of our work include (1) exploring the RNA binding interactions of less sterically demanding porphyrins, (2) bringing luminescence results to bear on the problem, and (3) expanding the library of viable RNA hosts. The analysis to follow focuses on limiting spectra, i.e., those obtained under conditions of relatively high host concentrations. Aside from simplifying the discussion, these are conditions of choice, because a relatively low ligand concentration is apt to mimic physiological conditions. In addition, the host−guest interaction itself shapes the binding in this loading regime.

Cu(*t*D4) and Cu(*c*D4) are less bulky than Cu(T4) because they bear only half as many substituents. Steric requirements may be such that intercalation of a bulky ligand is incompatible with the normal double helix. On the other hand, base stacking and the hydrogen bonding framework favor retention of the duplex structure. The competition is such that the binding motif can be base-dependent. Thus, relatively rigid DNA hosts rich in G≡C base pairs support the intercalation of H_2T4 or Cu(T4).[10,11] On the other hand, within A═T rich sequences, structural reorganization takes place more easily, and the bulky porphyrins shift to external binding. In the case of sterically friendly H_2*t*D4, however, previous work has shown that the porphyrin intercalates into DNA regardless of the base composition.[41] Absorbance and emission data in Table 3 pertaining to DNA hairpins CG[t_4] and TT[t_4] suggest that Cu(*t*D4) is also a universal intercalator. Intercalation presents a lesser steric problem for H_2*t*D4 or Cu(*t*D4) because only one pyridiniumyl substituent has to reside in the minor groove. Additional results in Table 3 suggest that Cu(*c*D4) also binds to DNA strictly by intercalation. In this case, however, the orientation with respect to the DNA host is uncertain because of the *cis* relationship of the substituents. Thus, Cu(*c*D4) can intercalate with one substituent in each groove or with both substituents in the same groove.

Interpretation of RNA Binding Interactions. The evidence is unmistakable that the RNA hosts strictly internalize each of the copper(II) porphyrins, almost certainly within the stem domains. End capping at the 5′ end of the hairpin cannot, for example, explain the lack of solvent exposure. Loop binding is equally improbable because the 5′-CuucgG-3′ hairpin fold is so compact and self-integrated, showing limited reactivity with single-strand-specific nucleases.[60] Encapsulation of a porphyrin in the loop domain would require an induced fit predicated on significant reorganization of the structure; however, introducing more duplex-stabilizing G≡C base pairs enhances the fit, as reflected by the emission intensity. In light of the G≡C dependence of the emission intensity and the extent of hypochromism, there is little doubt but that the host sandwiches the ligand within the stem domain instead and thus shields the copper(II) center from solvent attack. It is quite remarkable that the binding motif does not depend on the base composition, even for the bulky Cu(T4) system. Indeed, the hypochromic responses and emission intensities obtained with Cu(T4) and A═U rich hosts compare favorably with the responses found for the CG[t_4] DNA. The compactness of the porphyrin nevertheless remains a factor because sterically friendly porphyrins always exhibit stronger emission signals, doubtlessly because they pack into the binding cavity more efficiently. Solvent accessible channels or transient breathing motions of the host inevitably leave the copper center at least partially exposed.

The anomalously high emission intensity sometimes evident at higher loadings (low q values) has another basis. Figure 7 reveals an outstanding example as it shows unusually strong emission from Cu(*c*D4) bound to RNA hairpin A-GUAU at q = 3. Note that under the same conditions the system also exhibits a strong hypochromic effect (Figure 6). Both effects track with each other and diminish in amplitude with the addition of more RNA until the limiting spectra develop. An early phase of outside stacking could potentially explain the transient hypochromism but is inconsistent with the strong emission signal present when q = 3. A more likely explanation is that the strong hypochromism is due to exciton coupling of near neighbor porphyrins bound to the same hairpin.[42] The anomalously strong emission can then be traced to the loss of fluidity that occurs when the stem takes up more than one ligand.

In view of the unchanging binding motif, the induced CD signals are remarkably variable. As with acridine orange,[50] the sign of the signal differs depending on whether the dipyridiniumyl porphyrin binds to an RNA or a DNA host. More specifically, intercalation of Cu(*c*D4) or Cu(*t*D4) into ds RNA induces a positive CD signal. In contrast, the signal is negative when Cu(T4) binds to an A═U rich RNA host and bisignate if the host is rich in G≡C base pairs. External self-stacking of the porphyrin could give rise to a conservative, bisignate CD signal but would not account for the observed emission signal. A more plausible possibility is that the induced CD signal from Cu(T4) is intrinsically bisignate because the two components of the doubly degenerate excited state respond differently within the asymmetric environment.[61] This explanation is appealing because the same low-symmetry effect also accounts for the splitting that occurs in the Soret absorption when Cu(*t*D4) binds by intercalation. Symmetry lowering by peripheral substitution alone does not lead to a splitting of the Soret transition;[62] however, exciton coupling to base-centered excitations could be highly directional within an

dx.doi.org/10.1021/bi300828z | *Biochemistry* 2012, 51, 7496−7505

intercalation site. For any given porphyrin, other variations in the induced CD spectrum could arise from local departures from canonical structure. Intercalation always requires cavity formation and helix unwinding,[45,63] but effects like extrusion of the base from the duplex may also be necessary to accommodate a sterically demanding ligand.[39]

In summary, a crystal structure shows that the copper center of Cu(*t*D4) is four-coordinate. The absence of axial ligands facilitates intercalation and sets the stage for solvent-assisted quenching of the emission. Double-stranded domains of hairpin-forming RNA sequences allow for base pair variations and are useful for binding studies of Cu(*t*D4) and other cationic porphyrins. In conjunction with strong hypochromism, the unique emissive properties of copper-containing forms establish that intercalation is the preferred binding motif not only for sterically friendly dicationic porphyrins but also for the bulky Cu(T4) system. Regardless of base content, A-form RNA actually proves to be more adept at internalizing cationic porphyins than B-form DNA. Bound forms of compact porphyrins like dipyridiniumyl Cu(*t*D4) are less prone to axial attack, on the time scale of the excited-state lifetime, and intercalation of Cu(*t*D4) in particular induces an unusual splitting of the Soret band. Minor differences in the binding interactions are responsible for significant differences in the induced CD spectra. Indeed, $\Delta\varepsilon$ is opposite in sign for the Soret bands of Cu(T4) and Cu(*t*D4), even though both porphyrins intercalate into ds RNA. The exquisite sensitivity may be due to the fact that the CD response depends on the base arrangement within the host as well as ligand placement relative to the base pairs. More work will be necessary to elucidate all the details.

■ ASSOCIATED CONTENT

Supporting Information

Experimental details regarding methylation, copper insertion, and aggregation studies of porphyrins and four figures of spectral data mentioned in the text. This material is available free of charge via the Internet at http://pubs.acs.org. File CCDC 859673 (CUTD4), which contains the crystallographic data, is available from the Cambridge Crystallographic Data Centre via http://www.ccdc.cam.ac.uk/data_request/cif.

■ AUTHOR INFORMATION

Corresponding Author

*E-mail: mcmillin@purdue.edu. Phone: (765) 494-5452.

Funding

The National Science Foundation funded this research via Grant CHE 0847229.

Notes

The authors declare no competing financial interest.

■ ACKNOWLEDGMENTS

We are grateful to Professor Barbara Golden for valuable discussions and assistance. Dr. Marcin Ptaszek also provided help with porphyrin synthesis.

■ ABBREVIATIONS

H_2T4, 5,10,15,20-tetrakis(*N*-methylpyridinium-4-yl)porphyrin; Cu(T4), [5,10,15,20-tetrakis(*N*-methylpyridinium-4-yl)-porphyrinato]copper(II); H_2*c*D4, 5,10-di(*N*-methylpyridinium-4-yl)porphyrin; Cu(*t*D4), [*trans*-5,15-di(*N*-methylpyridinium-4-yl)porphyrinato]copper(II); Cu(*c*D4), [*cis*-5,10-di(*N*-methylpyridinium-4-yl)porphyrinato]copper(II); CD, circular dichroism; MeCN, acetonitrile; DDQ, 2,3-dichloro-5,6-dicyano-1,4-benzoquinone; DMF, *N*,*N*-dimethylformamide; DCM, dichloromethane; HNO_3, nitric acid; TEMED, *N*,*N*,*N*′,*N*′-tetramethylethylene diamine; $Cu(OAc)_2$, copper(II) acetate; CH_3I, methyl iodide; TBAN, tetrabutylammonium nitrate; KPF_6, potassium hexafluorophosphate; ds, double-stranded; MeOH, methanol; *q*, ratio of base pair concentration with respect to porphyrin concentration.

■ REFERENCES

(1) Ali, H., and van Lier, J. E. (1999) Metal complexes as photo- and radiosensitizers. *Chem. Rev. 99*, 2379−2450.
(2) Henderson, B. W., and Dougherty, T. J. (1992) How Does Photodynamic Therapy Work. *Photochem. Photobiol. 55*, 145−157.
(3) Griffiths, J. (2004) Colourful Therapy. *Educ. Chem. 41*, 71−73.
(4) Snyder, J. W., Skovsen, E., Lambert, J. D. C., and Ogilby, P. R. (2005) Subcellular, time-resolved studies of singlet oxygen in single cells. *J. Am. Chem. Soc. 127*, 14558−14559.
(5) Han, F. X. G., Wheelhouse, R. T., and Hurley, L. H. (1999) Interactions of TMPyP4 and TMPyP2 with quadruplex DNA. Structural basis for the differential effects on telomerase inhibition. *J. Am. Chem. Soc. 121*, 3561−3570.
(6) Fiel, R. J., and Munson, B. R. (1980) Binding of Meso-Tetra(4-N-Methylpyridyl) Porphine to DNA. *Nucleic Acids Res. 8*, 2835−2842.
(7) Carvlin, M. J., and Fiel, R. J. (1983) Intercalative and Nonintercalative Binding of Large Cationic Porphyrin Ligands to Calf Thymus DNA. *Nucleic Acids Res. 11*, 6121−6139.
(8) Carvlin, M. J., Dattagupta, N., and Fiel, R. J. (1982) Circular-Dichroism Spectroscopy of a Cationic Porphyrin Bound to DNA. *Biochem. Biophys. Res. Commun. 108*, 66−73.
(9) Fiel, R. J. (1989) Porphyrin-Nucleic-Acid Interactions: A Review. *J. Biomol. Struct. Dyn. 6*, 1259−1275.
(10) Pasternack, R. F., and Gibbs, E. J. (1996) Porphyrin and metalloporphyrin interactions with nucleic acids. *Met. Ions Biol. Syst. 33*, 367−397.
(11) Marzilli, L. G. (1990) Medical Aspects of DNA-Porphyrin Interactions. *New J. Chem. 14*, 409−420.
(12) McMillin, D. R., and McNett, K. M. (1998) Photoprocesses of copper complexes that bind to DNA. *Chem. Rev. 98*, 1201−1219.
(13) Wimberly, B., Varani, G., and Tinoco, I. (1993) The Conformation of Loop-E of Eukaryotic 5S-Ribosomal RNA. *Biochemistry 32*, 1078−1087.
(14) Blose, J. M., Proctor, D. J., Veeraraghavan, N., Misra, V. K., and Bevilacqua, P. C. (2009) Contribution of the Closing Base Pair to Exceptional Stability in RNA Tetraloops: Roles for Molecular Mimicry and Electrostatic Factors. *J. Am. Chem. Soc. 131*, 8474−8484.
(15) Wadkins, R. M. (2000) Targeting DNA secondary structures. *Curr. Med. Chem. 7*, 1−15.
(16) Meister, G. (2008) Molecular biology: RNA interference in the nucleus. *Science 321*, 496−497.
(17) Fire, A., Xu, S. Q., Montgomery, M. K., Kostas, S. A., Driver, S. E., and Mello, C. C. (1998) Potent and specific genetic interference by double-stranded RNA in *Caenorhabditis elegans*. *Nature 391*, 806−811.
(18) Wilson, W. D., and Li, K. (2000) Targeting RNA with small molecules. *Curr. Med. Chem. 7*, 73−98.
(19) Aboul-Ela, F. (2010) Strategies for the design of RNA-binding small molecules. *Future Med. Chem. 2*, 93−119.
(20) Wilson, W. D., Ratmeyer, L., Zhao, M., Strekowski, L., and Boykin, D. (1993) The Search for Structure-Specific Nucleic-Acid Interactive Drugs: Effects of Compound Structure on RNA Versus DNA Interaction Strength. *Biochemistry 32*, 4098−4104.
(21) Uno, T., Aoki, K., Shikimi, T., Hiranuma, Y., Tomisugi, Y., and Ishikawa, Y. (2002) Copper insertion facilitates water-soluble porphyrin binding to rA·rU and rA·dT base pairs in duplex RNA and RNA·DNA hybrids. *Biochemistry 41*, 13059−13066.
(22) Biver, T., Secco, F., and Venturini, M. (2005) Relaxation kinetics of the interaction between RNA and metal-intercalators: The

Poly(A)·Poly(U)/platinum-proflavine system. *Arch. Biochem. Biophys. 437*, 215−223.
(23) Islam, M. M., Chowdhury, S. R., and Kumar, G. S. (2009) Spectroscopic and Calorimetric Studies on the Binding of Alkaloids Berberine, Palmatine and Coralyne to Double Stranded RNA Polynucleotides. *J. Phys. Chem. B 113*, 1210−1224.
(24) Ghazaryan, A. A., Dalyan, Y. B., Haroutiunian, S. G., Tikhomirova, A., Taulier, N., Wells, J. W., and Chalikian, T. V. (2006) Thermodynamics of interactions of water-soluble porphyrins with RNA duplexes. *J. Am. Chem. Soc. 128*, 1914−1921.
(25) Lewis, F. D., Zhu, H. H., Daublain, P., Fiebig, T., Raytchev, M., Wang, Q., and Shafirovich, V. (2006) Crossover from superexchange to hopping as the mechanism for photoinduced charge transfer in DNA hairpin conjugates. *J. Am. Chem. Soc. 128*, 791−800.
(26) Nutiu, R., and Li, Y. F. (2004) Structure-switching signaling aptamers: Transducing molecular recognition into fluorescence signaling. *Chem.—Eur. J. 10*, 1868−1876.
(27) Eggleston, M. K., Crites, D. K., and McMillin, D. R. (1998) Studies of the base-dependent binding of Cu(T4) to DNA hairpins (H_2T4 = meso-tetrakis(4-(N-methylpyridiumyl))porphyrin). *J. Phys. Chem. A 102*, 5506−5511.
(28) Lugo-Ponce, P., and McMillin, D. R. (2000) DNA-binding studies of Cu(T4), a bulky cationic porphyrin. *Coord. Chem. Rev. 208*, 169−191.
(29) Thomas, K. E., and McMillin, D. R. (2001) Competitive binding studies of H_2T4 with DNA hairpins (H_2T4 = meso-tetrakis(4-(N-methylpyridiniumyl))porphyrin). *J. Phys. Chem. B 105*, 12628−12633.
(30) Boger, D. L., Fink, B. E., Brunette, S. R., Tse, W. C., and Hedrick, M. P. (2001) A simple, high-resolution method for establishing DNA binding affinity and sequence selectivity. *J. Am. Chem. Soc. 123*, 5878−5891.
(31) Monjardet-Bas, V., Bombard, S., Chottard, J. C., and Kozelka, M. (2003) GA and AG sequences of DNA react with cisplatin at comparable rates. *Chem.—Eur. J. 9*, 4739−4745.
(32) Zhang, J., Umemoto, S., and Nakatani, K. (2010) Fluorescent Indicator Displacement Assay for Ligand-RNA Interactions. *J. Am. Chem. Soc. 132*, 3660−3661.
(33) Krishnamurthy, M., Simon, K., Orendt, A. M., and Beal, P. A. (2007) Macrocyclic helix-threading peptides for targeting RNA. *Angew. Chem., Int. Ed. 46*, 7044−7047.
(34) Weng, X. C., Huang, J., Wu, S., Ren, L. G., Weng, L. W., Zhu, S. G., and Zhou, X. (2007) Specific recognition of loop DNA by dicationic Porphyrins. *Chem. Biodiversity 4*, 1501−1507.
(35) Molinaro, M., and Tinoco, I. (1995) Use of Ultra-Stable UNCG Tetraloop Hairpins to Fold RNA Structures-Thermodynamic and Spectroscopic Applications. *Nucleic Acids Res. 23*, 3056−3063.
(36) Duchardt, E., and Schwalbe, H. (2005) Residue specific ribose and nucleobase dynamics of the cUUCGg RNA tetraloop motif by NMR C-13 relaxation. *J. Biomol. NMR 32*, 295−308.
(37) Saenger, W. (1984) *Principles of Nucleic Acids Structure*, Springer-Verlag, New York.
(38) Lee, S. J., Hyun, S., Kieft, J. S., and Yu, J. (2009) An Approach to the Construction of Tailor-Made Amphiphilic Peptides That Strongly and Selectively Bind to Hairpin RNA Targets. *J. Am. Chem. Soc. 131*, 2224−2230.
(39) Lipscomb, L. A., Zhou, F. X., Presnell, S. R., Woo, R. J., Peek, M. E., Plaskon, R. R., and Williams, L. D. (1996) Structure of a DNA−porphyrin complex. *Biochemistry 35*, 2818−2823.
(40) Wall, R. K., Shelton, A. H., Bonaccorsi, L. C., Bejune, S. A., Dube, D., and McMillin, D. R. (2001) H_2D3: A cationic porphyrin designed to intercalate into B-form DNA (H_2D3 = trans-di(N-methylpyridium-3-yl)porphyrin). *J. Am. Chem. Soc. 123*, 11480−11481.
(41) Bejune, S. A., Shelton, A. H., and McMillin, D. R. (2003) New dicationic porphyrin ligands suited for intercalation into B-form DNA. *Inorg. Chem. 42*, 8465−8475.
(42) Shelton, A. H., Rodger, A., and McMillin, D. R. (2007) DNA binding studies of a new dicationic porphyrin. Insights into interligand interactions. *Biochemistry 46*, 9143−9154.
(43) Wu, S., Wang, P., Tian, T., Wu, L., He, H. P., Zhou, X. A., Zhang, X. L., and Cao, X. P. (2004) Peripheral substituents of di(pyridiumyl)porphyrins affected on their interactions with DNA. *Bioorg. Med. Chem. Lett. 14*, 2575−2577.
(44) Wu, S., Li, Z., Ren, L. G., Chen, B., Liang, F., Zhou, X., Jia, T., and Cao, X. P. (2006) Dicationic pyridium porphyrins appending different peripheral substituents: Synthesis and studies for their interactions with DNA. *Bioorg. Med. Chem. 14*, 2956−2965.
(45) McMillin, D. R., Shelton, A. H., Bejune, S. A., Fanwick, P. E., and Wall, R. K. (2005) Understanding binding interactions of cationic porphyrins with B-form DNA. *Coord. Chem. Rev. 249*, 1451−1459.
(46) Sambrook, J., Fritsch, E. F., and Maniatis, T. (1989) *Molecular Cloning: A Laboratory Manual*, 2nd ed., Vol. 3, Cold Spring Harbor Laboratory Press, Plainview, NY.
(47) Dogutan, D. K., and Lindsey, J. S. (2008) Investigation of the scope of a new route to ABCD-bilanes and ABCD-porphyrins. *J. Org. Chem. 73*, 6728−6742.
(48) Batinic-Haberle, I., Spasojevic, I., Hambright, P., Benov, L., Crumbliss, A. L., and Fridovich, I. (1999) Relationship among redox potentials, proton dissociation constants of pyrrolic nitrogens, and in vivo and in vitro superoxide dismutating activities of manganese(III) and iron(III) water-soluble porphyrins. *Inorg. Chem. 38*, 4011−4022.
(49) Cantor, C. R., Warshaw, M. M., and Shapiro, H. (1970) Oligonucleotide Interactions. 3. Circular Dichroism Studies of Conformation of Deoxyribonucleotides. *Biopolymers 9*, 1059−1077.
(50) Zama, M., and Ichimura, S. (1976) Induced Circular Dichroism of Acridine Orange Bound to Double-Stranded RNA and Transfer RNA. *Biopolymers 15*, 1693−1699.
(51) Demas, J. N., and Crosby, G. A. (1971) Measurement of Photoluminescence Quantum Yields: Review. *J. Phys. Chem. 75*, 991−1024.
(52) Pasternack, R. F., and Cobb, M. A. (1973) Substitution Reactons of a Water-Soluble Cobalt(III) Porphyrin with Thiocyanate as a Function of pH. *J. Inorg. Nucl. Chem. 35*, 4327−4339.
(53) Sheldrick, G. M. (2008) A short history of SHEL. *Acta Crystallogr. A64*, 112−122.
(54) Sari, M. A., Battioni, J. P., Mansuy, D., and Lepecq, J. B. (1986) Mode of Interaction and Apparent Binding Constants of Meso-Tetraaryl Porphyrins Bearing between One and Four Positive Charges with DNA. *Biochem. Biophys. Res. Commun. 141*, 643−649.
(55) Strickland, J. A., Marzilli, L. G., and Wilson, W. D. (1990) Binding of Meso-Tetrakis(N-Methylpyridiniumyl)Porphyrin Isomers to DNA: Quantitative Comparison of the Influence of Charge-Distribution and Copper(II) Derivatization. *Biopolymers 29*, 1307−1323.
(56) Zama, M., and Ichimura, S. (1970) Circular Dichroism of Acridine Orange Bound to DNA. *Biopolymers 9*, 53−63.
(57) Hudson, B. P., Sou, J., Berger, D. J., and McMillin, D. R. (1992) Luminescence Studies of the Intercalaton of Cu(TMpyP4) into DNA. *J. Am. Chem. Soc. 114*, 8997−9002.
(58) Kelly, J. M., Murphy, M. J., McConnell, D. J., and Ohuigin, C. (1985) A Comparative Study of the Interaction of 5,10,15,20-Tetrakis(N-Methylpyridinium-4-yl)Porphyrin and its Zinc Complex with DNA Using Fluorescence Spectroscopy and Topisomerization. *Nucleic Acids Res. 13*, 167−184.
(59) Barnes, N. R., Schreiner, A. F., and Dolan, M. A. (1998) Measurement and interpretation of Q(0) and Q(1) band property changes of two cationic metalloporphyrins upon binding with B-DNA: Electronic MCD, CD, and optical absorption. *J. Inorg. Biochem. 72*, 1−12.
(60) Varani, G., Cheong, C. J., and Tinoco, I. (1991) Structure of an Unusually Stable RNA Hairpin. *Biochemistry 30*, 3280−3289.
(61) Berova, N., and Nakanishi, K. (2000) Exciton Chirality Method: Principles and Applications. In *Circular Dichroism: Principles and Applications* (Nakanishi, K., Berova, N., and Woody, R., Eds.) 2nd ed., pp 337−382, Wiley-VCH, New York.
(62) Gouterman, M. (1959) Study of the Effects of Substitution on the Absorption Spectra of Porphin. *J. Chem. Phys. 30*, 1139−1161.

(63) Calladine, C. R., and Drew, H. R. (1997) *Understanding DNA*, Academic Press, New York.